

On the Gelation of Graphene Oxide

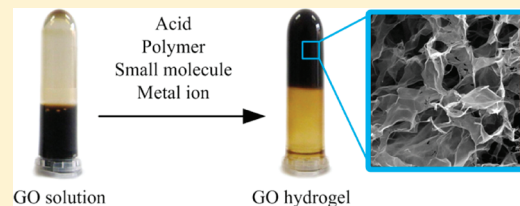
Hua Bai,^{†,‡} Chun Li,[†] Xiaolin Wang,[‡] and Gaoquan Shi^{*,†}

[†]Key Laboratory of Bio-organic Phosphorous Chemistry and Chemical Biology, Tsinghua University, Beijing, 100084, People's Republic of China

[‡]Department of Chemical Engineering, Tsinghua University, Beijing, 100084, People's Republic of China

 Supporting Information

ABSTRACT: Graphene oxide (GO) has been recognized as a unique two-dimensional building block for various graphene-based supramolecular architectures. In this article, we systematically studied the three-dimensional self-assembly of GO sheets in aqueous media to form hydrogels. The gelation of GO can be promoted by different supramolecular interactions, including hydrogen bonding, π -stacking, electrostatic interaction, and coordination. Furthermore, the lateral dimensions of GO sheets also have strong influences on GO gelation. The resulting GO hydrogels exhibited low critical gelation concentrations and good reversibility upon chemical stimulations. These findings indicate that GO has rich supramolecular properties, and its hydrogels may have a variety of technological applications.



■ INTRODUCTION

In the past half decade, graphene oxide (GO), a precursor of graphene,^{1–4} has attracted a great deal of attention due to its unique structure and outstanding physical and chemical properties.^{5–8} Particularly, GO behaves like an amphiphilic macromolecule with hydrophilic edges and a more hydrophobic basal plane,^{9–11} which makes it an attractive building block for the construction of various supramolecular architectures.^{12,13} Furthermore, the two-dimensional (2D) structure of GO sheets provides them with various new supramolecular behaviors compared with conventional low-dimensional counterparts. Although GO sheets have been assembled into various macrostructures, such as Langmuir–Blodgett (LB) films and paper-like films,^{14–17} their 3D assembly behavior has not yet been clearly revealed.¹⁸ We have first reported the 3D assembly of GO sheets in water solution by adding poly(vinyl alcohol) (PVA) as a cross-linker, forming a pH-sensitive supramolecular hydrogel.¹⁹ Hydrogen bonding between GO sheets and PVA chains is believed to be responsible for the formation of the hydrogel. Recently, single-stranded DNA was also found to be a good cross-linker for preparing a GO/DNA composite hydrogel, in which π – π interaction was the dominant driving force.²⁰ Similarly, hydrogels based on chemically concerted graphene (CCG) have also been reported by us and other groups.^{21–25} These examples reflect that GO and CCG are good gelators. However, the gelation of GO sheets has not yet been studied extensively and the fundamental roles behind gelation phenomena have also not been clearly revealed. Here, we report a systematical study on GO gelation. The GO-based hydrogels were prepared by acidification or adding small organic molecules, polymers, or ions as cross-linkers. The effects of different driving forces (e.g., hydrogen bonding, electrostatic interaction, and coordination) and lateral dimensions of GO sheets on GO gelation are discussed.

■ EXPERIMENTAL SECTION

Natural graphite powders were bought from Qingdao Huatai lubricant sealing S&T Co. Ltd. (Qingdao, China). Poly(vinyl pyrrolidone) (PVP), poly(ethylene oxide) (PEO), polydimethylidiallylammonium chloride (PDDA), polyethylenimine (PEI), cetyltrimethyl ammonium bromide (CTAB), tetramethylammonium chloride (TMAC), and melamine were the products of Alfa Aesar. Ethylene diamine tetraacetic acid disodium salt (Na_2EDTA) was purchased from Biosharp Co. Ltd. All the inorganic salts, including NaCl , KCl , AgNO_3 , CaCl_2 , MgCl_2 , CuCl_2 , $\text{Pb}(\text{NO}_3)_2$, CrCl_3 , and FeCl_3 , were purchased from Sinopharm Chemical Reagents Co. Ltd. (Beijing, China). All the chemicals were used as received without further purification.

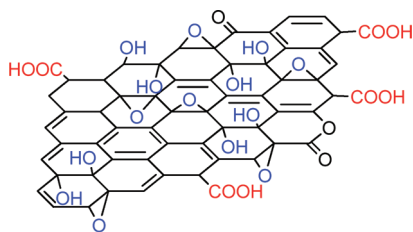
GO was prepared from natural graphite powder by a modified Hummers method^{26,27} and purified by dialysis for 1 week to remove any impurities. Natural graphite with average particle sizes of 325 and 12 000 mesh were used for synthesizing GO sheets with larger and smaller lateral dimensions, respectively. To prepare GO hydrogels, a certain volume GO dispersion was mixed with the solution of acid or other cross-linkers. The blend was then shaken violently for several seconds to form a hydrogel. The formation of the hydrogel was examined by a tube inversion method, in which a polypropylene tube with an inner diameter of 8 mm was used.

Atomic force micrographs (AFMs) were recorded on a Nanoscope III MultiMode SPM (Digital Instruments) with an AS-12 ("E") scanner operated in tapping mode in conjunction with a V-shaped tapping tip (Applied Nanostructures SPM model: ACTA). The images were taken out at a scan rate of

Received: December 17, 2010

Revised: January 27, 2011

Published: March 14, 2011

Scheme 1. Chemical Structure of GO^a

^a Hydrophilic groups are colored in red (carboxyl groups) and blue (hydroxyl and epoxy groups).

2 Hz. X-ray diffraction (XRD) was carried out using a D8 Advance (Bruker) X-ray diffractometer with Cu K α radiation ($\lambda = 1.5418 \text{ \AA}$). All the GO solutions and hydrogels were lyophilized for at least 24 h before XRD measurement. Scanning electron micrographs (SEMs) were taken out by the use of a FEI Quanta 200 scanning electron microscope. Rheological studies were performed on an MCR 300 (Paar Physica) rheometer. All the viscosity data were obtained by using a 25 mm diameter parallel plate with a 1 mm plate–plate gap.

RESULTS AND DISCUSSION

A GO sheet can be regarded as a single-layer graphite that brings various hydrophilic oxygenated functional groups (Scheme 1).^{28–30} Thus, GO sheets can be dispersed in water to form a stable colloidal dispersion. It was also believed that the electrostatic repulsion between GO sheets, resulting from their ionized carboxyl groups, prevented their aggregation in aqueous medium.³¹ Therefore, acidification of a GO dispersion would weaken the electrostatic repulsion and lead to the formation of a graphite oxide flocculent. This phenomenon was observed by us as well as other researchers. The ζ potential of a GO dispersion increases with the decrease of its pH value, indicating the protonation of carboxyl groups (Figure 1A). Therefore, GO sheets are unstable in a strong acidic aqueous medium because of insufficient mutual repulsion.³² However, as the concentration of GO (C_{GO}) was sufficiently high ($>4 \text{ mg mL}^{-1}$), a hydrogel instead of an amorphous precipitation formed upon acidification. Figure 1A also gives the zero-shear viscosities (η_0) of a 5 mg mL⁻¹ GO solution at different pH values. Because of the ionization of carboxyl groups, the initial GO solution is acidic (pH = 4.6). Increasing the pH value of the GO solution using NaOH slightly decreased its η_0 , owing to the increase of the repulsion force between GO sheets. However, when the pH value of the GO solution was lowered from 4.6 to 0.6 by adding hydrochloric acid, its η_0 increased dramatically from 290 to 10 850 Pa s. As a result, a hydrogel quickly formed within several seconds, indicating the generation of a 3D infinite network in the solution. The formation of the hydrogel was tested to be independent of the types of acids used for acidification. Thus, the 3D GO network must have resulted from the self-assembly of acidified GO sheets. In this case, the electrostatic repulsion between GO sheets was weakened and their hydrogen-bonding force was enhanced due to the protonation of carboxyl groups. Further lowering the pH value (<0.6) led to the precipitation of GO sheets and decreased the η_0 of the dispersion. Figure 1B (black line) shows the concentration dependence of η_0 of the GO dispersion at pH = 0.6 (the corresponding dynamic rheological test results are shown in Figure S1 (Supporting

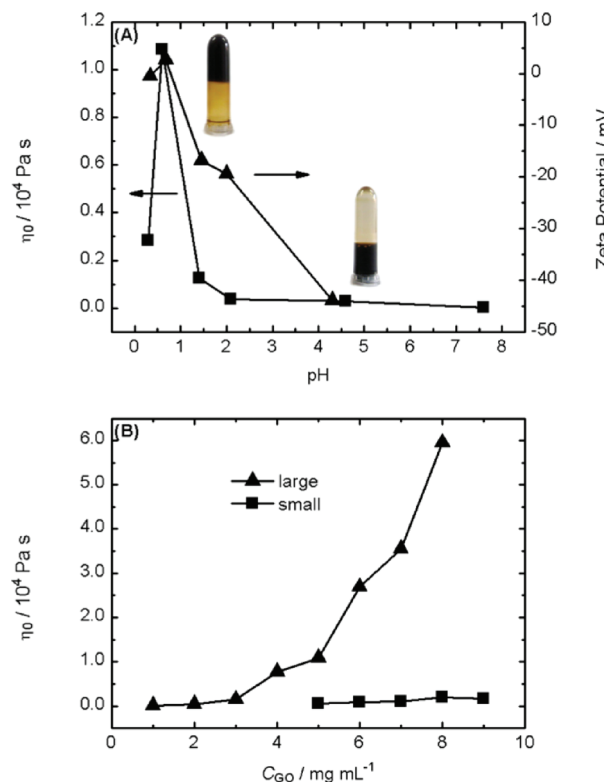


Figure 1. (A) Zero-shear viscosities and ζ potentials of a GO aqueous solution ($C_{\text{GO}} = 5 \text{ mg mL}^{-1}$) at different pH values. The insets show the photographs of a GO solution at pH = 4.6 and a hydrogel at pH = 0.6. (B) Zero-shear viscosities of the solutions of GO sheets with large (>2 μm) and small (<1 μm) lateral dimensions; pH = 0.6.

Information)). It is clear from this figure that η_0 increases slightly with the increase of C_{GO} as $C_{\text{GO}} < 3 \text{ mg mL}^{-1}$. In contrast, η_0 increases dramatically with C_{GO} in the region of $C_{\text{GO}} > 3 \text{ mg mL}^{-1}$. At 4 mg mL⁻¹, a stable hydrogel was formed, as confirmed by the tube inversion method. This is a rather low critical gel concentration (CGC), indicating that GO falls into the concept of “super gelator”.³³

An essential difference between GO sheets and conventional amphiphilic molecules is that GO sheets have much larger lateral dimensions. Furthermore, we found that the lateral dimensions of GO sheets have strong effects on their gelation behavior. For example, as the lateral dimensions of most GO sheets are as large as several micrometers (Figure 2A), a stable hydrogel can be easily formed by acidification (Figure 1A). Decreasing the lateral dimension of GO sheets is unfavorable for GO gelation. Actually, if the lateral dimensions of most GO sheets are smaller than 1 μm (Figure 2B), no gelation occurred at any pHs even if the C_{GO} was as high as 9 mg mL⁻¹ (Figure 1B). In this case, the acidified solutions of small GO sheets turned cloudy in several minutes, indicating the occurrence of GO precipitation. Therefore, the lateral dimension of GO sheets is a key factor for deciding their gelating ability.

The size effect described above can be explained as follows. To some extent, GO can be regarded as an amphiphilic macromolecule. However, the sizes of large GO sheets (several micrometers) are much larger than those of conventional polymers. Therefore, they can contact with each other even in a dilute solution. This assumption was confirmed by the fact that the

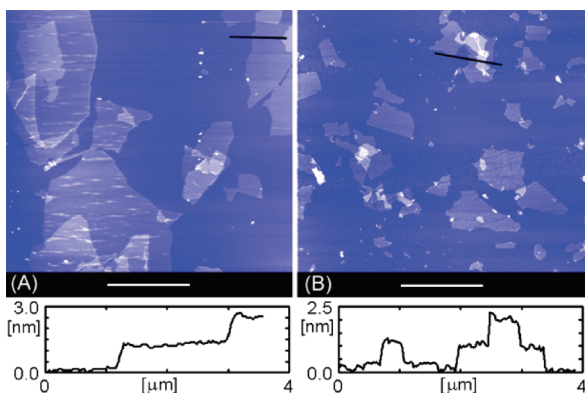


Figure 2. AFM images of two GO samples with different average lateral dimensions. Scale bar = 5 μm .

freeze-dried sample of a 3 mg mL^{-1} GO dispersion can maintain the original volume of the solution. In contrast, lyophilizing a 3 mg mL^{-1} PVA (Scheme 2) produced a shrunken sample (Figure S2, Supporting Information). Furthermore, the lyophilized GO dispersion shows a 3D network composed of GO sheets, as shown by its SEM image (Figure 3A). Therefore, it is reasonable to conclude that a loose dynamic GO network existed in the original dispersion of GO sheets owing to a force balance between electrostatic repulsion and binding interactions (hydrogen bonding, π -stacking, hydrophobic effect, etc.). Gelation occurs as the GO network in solution is reinforced by enhancing the bonding force or weakening the repulsion force. Acidification is an effective way for this purpose, as described above. On the other hand, both gelation and precipitation of GO sheets can be induced by reinforcing their bonding interaction. The difference between a GO hydrogel and graphite oxide precipitation is the stacking states of their GO sheets. GO sheets are randomly orientated in a hydrogel, whereas they adopt a parallel arrangement in their precipitation. The latter staking mode is energetically favorable because of the larger contacting area between GO sheets. However, the mobility of large GO sheets in solution is strongly limited. As a result, it is difficult to adjust their orientation to be parallel with each other. Comparing with the gelation process, precipitation is a kinetically slower process. Moreover, the large conjugated basal planes make the GO sheets stiff and form a stable network. The conversion of the GO network to the energetically more stable state (precipitation) is rather slow. In fact, a very slow precipitation process was observed after 2 weeks of the formation of hydrogels. However, if the sizes of GO sheets were reduced, for example, to be smaller than 1 μm in our experiment, they can change their conformations and positions in solution more easily. Consequently, acidified GO sheets trend to aggregate in an energetically favorable layer-by-layer manner to form a precipitation. The stability of a hydrogel is decided by the strength ratio of repulsion and bonding forces between GO sheets. For example, over-acidification of the dispersion of large GO sheets would also lead to the formation of irregular aggregates because of too weak repulsion forces.

To reveal the gelation behaviors of GO sheets more extensively, we used the large GO sheets for preparing hydrogels in the following studies. According to the analyses described above, the addition of a cross-linker can increase the bonding force between GO sheets and consequently promote gelation. This deduction

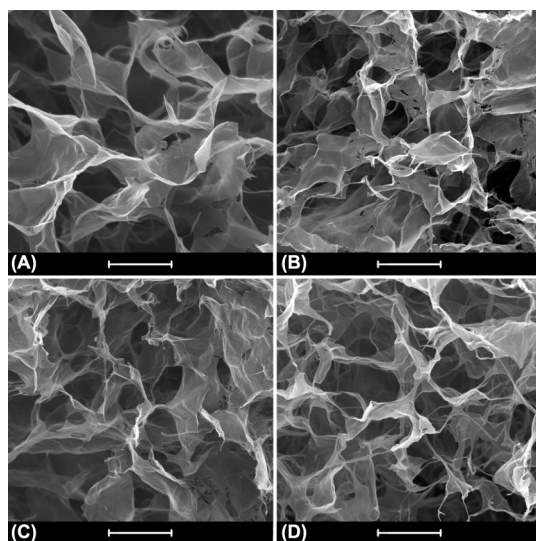


Figure 3. SEM images of lyophilized GO solution and three typical GO hydrogels: (A) GO solution, (B) GO/PVP hydrogel with 1 mg mL^{-1} PVP, (C) GO/PDDA hydrogel with 0.1 mg mL^{-1} PDDA, and (D) GO/ Ca^{2+} hydrogel with 9 mM Ca^{2+} . $C_{\text{GO}} = 5 \text{ mg mL}^{-1}$, and scale bar = 10 μm .

was first examined by introducing a polymer component to provide additional hydrogen-bonding interaction. In a previous work, we have reported that a small amount of PVA (<0.5 wt %) could induce the gelation of GO,¹⁹ owing to the hydrogen-bonding interaction between GO sheets and PVA chains. Actually, GO sheets can blend with many other polymers to form hydrogen bonds.^{34,35} In Figure 4, photos 1–3 show the hydrogels prepared by mixing small amounts of poly(ethylene oxide) (PEO, $M = 1\,000\,000$), hydroxypropylcellulose (HPC), and poly(vinyl pyrrolidone) (PVP, $M = 1\,300\,000$) (Scheme 2) into GO dispersions. Among these three polymers, PEO and PVP are hydrogen-bond acceptors, whereas HPC is both a hydrogen-bond donor and acceptor. Thus, they can form hydrogen bonds with adjacent GO sheets, providing an additional bonding force for the gelation of GO. All the GO/polymer composite hydrogels show 3D networks with a morphology similar to that of pure GO hydrogel (Figures 3B and S3 (Supporting Information)), indicating that the polymer additives did not change the conformation of GO sheets. However, as shown in Figure 5, the X-ray diffraction (XRD) patterns of lyophilized GO/PVP and GO/PEO hydrogels exhibit different features. All the XRD patterns of GO/PVP composites show a peak associated with GO sheets at the angle range of $2\theta = 10.5\text{--}12.5^\circ$. The position of this peak is close to that of pure GO sheets at $2\theta = 11.5^\circ$ (the interplanar distance of GO sheets was calculated to be 1.54 nm).³⁶ However, its intensity decreases remarkably, and its full width at half-maximum (fwhm) value increases simultaneously with the increase of PVP content (Figure 5A). This phenomenon has also been observed in the GO/carbon nanotube composite film³⁷ and can be explained by the intercalation between PVP chains and GO sheets. The XRD results indicated that the stacking of GO sheets was partly prevented by inducing PVP chains. However, the XRD peak of PVP intercalated GO sheets was not observed in the experimental angle scale, possibly due to their large d -space. However, if PEO was used as the cross-linker, the XRD peaks of the hydrogels shifted to smaller angles upon increasing their PEO contents (Figure 5B), which is similar to that of the GO/PVA hydrogel.¹⁹ The interplanar distance of GO

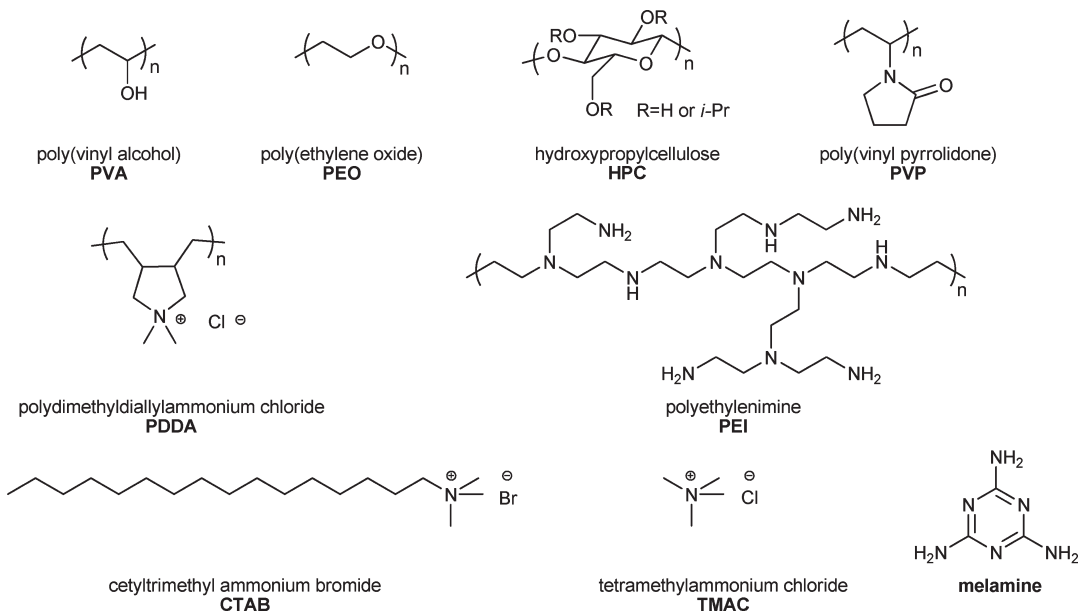
Scheme 2. Chemical Structures of Several Cross-Linkers Used to Prepare GO Composite Hydrogels

Figure 4. Photographs of 5 mg mL^{-1} GO solutions mixed with different cross-linkers: 1, 0.5 mg mL^{-1} PVP; 2, 1 mg mL^{-1} HPC; 3, 1 mg mL^{-1} PEO; 4, 0.1 mg mL^{-1} PDDA; 5, 0.2 mg mL^{-1} PEI; 6, 0.3 mg mL^{-1} CTAB; 7, 1.9 mg mL^{-1} TMAC; 8, 0.3 mg mL^{-1} melamine; 9, 20 mM Li^+ ; 10, 20 mM K^+ ; 11, 20 mM Ag^+ ; 12, 15 mM Mg^{2+} ; 13, 9 mM Ca^{2+} ; 14, 3 mM Cu^{2+} ; 15, 3 mM Pb^{2+} ; 16, 3 mM Cr^{3+} ; 17, 3 mM Fe^{3+} . All the concentrations labeled above are the CGCs of corresponding cross-linkers, except for 9, 10, and 11.

sheets increased from 1.54 nm in pure GO to 2.93 nm in the GO hydrogel containing 5 mg mL^{-1} PEO. These results imply that PEO chains were sandwiched between GO sheets. The gradual increase of the interplanar distance of GO sheets in the GO/PEO hydrogel indicates that the intercalated PEO chains have a smaller radius than that of PVP. A reasonable explanation is that PVP chains are more hydrophobic; thus, they adapted a more contracted conformation or formed aggregates in the aqueous medium.

The formation of GO/polymer composite hydrogels is controlled by several factors, including C_{GO} , pH value, and the concentration and molar mass of the polymer. The C_{GO} is crucial for the formation of a 3D GO infinite network. If the C_{GO} is lower than the CGC of the GO/polymer hydrogel, the intercontacts between GO sheets are insufficient for forming a stable network even in the presence of a cross-linker.²⁴ The CGC of GO for

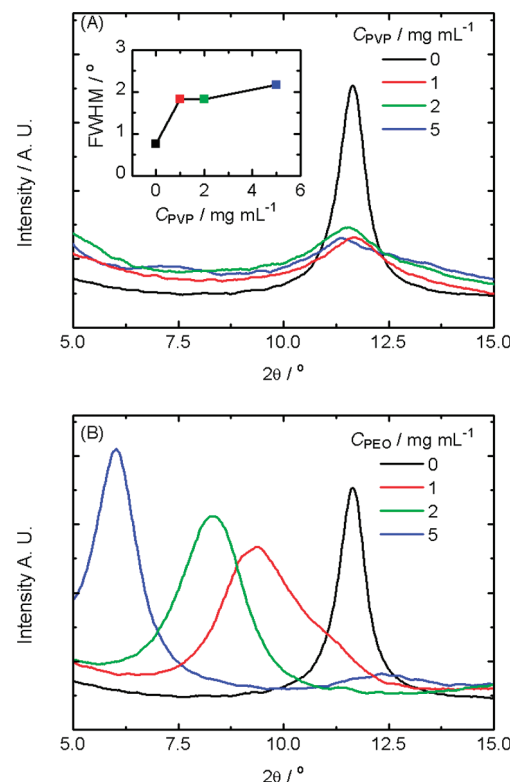


Figure 5. X-ray diffraction patterns of lyophilized GO, GO/PVP hydrogels (A), and GO/PEO hydrogels (B) ($C_{\text{GO}} = 5 \text{ mg mL}^{-1}$). The inset of (A) demonstrates the full width at half-maximum (fwhm) values of diffraction peaks of GO/PVP hydrogels containing different amounts of PVP.

GO/polymer hydrogels was measured to be about 3 mg mL^{-1} . Furthermore, the three GO/polymer hydrogels (GO/PVP, GO/HPC, GO/PEO) described above are pH-sensitive. They

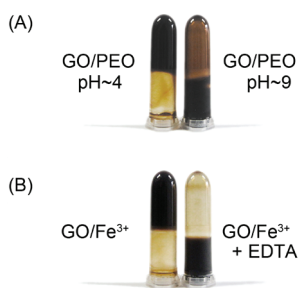


Figure 6. Photographs showing the gel–sol transitions of GO composite hydrogels: (A) GO/PEO (5 mg mL^{-1} GO and 1 mg mL^{-1} PEO) mixture at different pHs and (B) GO/Fe³⁺ (5 mg mL^{-1} GO and 3 mM Fe³⁺) hydrogel upon addition of 3 mM Na₂EDTA.

undergo gel–sol transitions upon increasing their pH values, and an example is given in Figure 6A. The SEM images of the lyophilized sample recorded before and after sol–gel transition do not show an apparent morphological difference (Figure S3, Supporting Information). Therefore, the sol–gel transition was not caused by the conformational change of GO sheets. Similar to the acid-induced GO hydrogel, this transition resulted from the increase of the electrostatic repulsion between GO sheets. As described above, the gelation of GO is controlled by the strength ratio of the electrostatic repulsion and the bonding force among GO sheets.

Thus, considering the difference in the bonding forces caused by different cross-linkers, one may design GO hydrogels with sol–gel transitions at various pHs. Apart from the two factors mentioned above, the molar mass of the polymer cross-linker is also expected to be able to influence the gelation process of GO hydrogels. We chose GO/PEO and GO/PVP hydrogels as the examples. As shown in Figure 7, the zero-shear viscosities of both hydrogels increase with the molar masses of cross-linkers. In fact, a longer polymer chain can form more hydrogen bonds with GO sheets and has a larger probability of interacting with two or more GO sheets. HPC was tested to be an effective cross-linker for the formation of a GO hydrogel, whereas monosaccharide glucose failed to act in this role because of its smaller molecular size. This observation also confirmed the molecular size effect on GO gelation described above.

Electrostatic interaction (ESI) is another driving force for supramolecular self-assembly, and the assembly of GO or graphene sheets induced by ESI has also been realized in many systems.^{38–40} To study the effect of ESI on GO gelation, polydimethylidiallylammonium chloride (PDDA, Scheme 2) was chosen as a model cross-linking agent for excluding the possibility of forming hydrogen bonds. In this case, ESI between the quaternary ammonium groups of PDDA and the carboxyl groups of GO sheets should be the dominating driving force for gelation. PDDA was tested to be an efficient cross-linker with a CGC as low as 0.1 mg mL^{-1} (Figure 4, photo 4). This value is much lower than those of PEO, PVP, and HPC, implying that ESI is more effective than hydrogen bonding for GO gelation. The microstructure of the GO/PDDA hydrogel is similar to that of the lyophilized GO dispersion (Figure 3C). In fact, the ESI between PDDA and GO is so strong that GO sheets were precipitated from their dispersion upon adding excess PDDA (for example, 0.5 mg mL^{-1}). This phenomenon was not observed in the GO/polymer gel systems formed by hydrogen bonding. To further confirm that ESI is an effective driving force

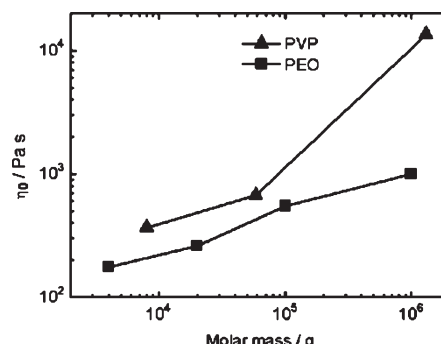


Figure 7. Zero-shear viscosities of two GO/polymer hydrogels each made from 5 mg mL^{-1} GO and 1 mg mL^{-1} polymer cross-linker with different molar masses.

for assembling GO sheets into hydrogels, polyethylenimine (PEI, Scheme 2) was used to replace PDDA as the cross-linking reagent. PEI chains bring primary, secondary, and tertiary amines, and most of these amino groups are protonated. Thus, hydrogen bonding and ESI coexist between GO sheets and PEI chains. PEI was examined to be a good cross-linker with a CGC of only 0.2 mg mL^{-1} (Figure 4, photo 5), and a higher concentration of PEI (0.5 mg mL^{-1}) also could induce GO precipitation. Therefore, polycations are a group of strong cross-linkers, but their concentrations need to be well-controlled to prevent GO precipitation. Interestingly, we found that small quaternary ammonium salts, such as cetyltrimethyl ammonium bromide (CTAB, Scheme 2) and tetramethylammonium chloride (TMAC, Scheme 2), could also promote the formation of GO hydrogels (Figure 4, photos 6 and 7). This is different from the case of using small molecules as hydrogen-bonding cross-linkers. This is mainly due to that ESI is a long-range force and it is usually stronger than that of a hydrogen bond. Moreover, CTAB was found to have a lower CGC value (0.3 mg mL^{-1}) than that of TMAC (1.9 mg mL^{-1}), indicating that the long hydrophobic chain on CTAB increased its interaction with GO sheets. Similarly, melamine (Scheme 2), a strong hydrogen-bond acceptor and multicharged small molecule in water, also exhibited good cross-linking ability with a CGC of only 0.3 mg mL^{-1} (Figure 4, photo 8).

It was reported that Ca²⁺ and Mg²⁺ ions could strengthen a layered GO paper by coordination with adjacent GO sheets.⁴¹ Interestingly, it was found that this cross-linking effect could also be realized in solution. Like the cross-linkers described above, a variety of metal ions can induce the gelation of GO solutions. The pictures 9–17 in Figure 4 are the photographs of GO dispersions after adding different metals ions. It is clear from these pictures that monovalent ions (e.g., K⁺, Li⁺, Ag⁺) cannot induce GO gelation, whereas divalent and trivalent ions (e.g., Ca²⁺, Mg²⁺, Cu²⁺, Pb²⁺, Cr³⁺, Fe³⁺) can promote the formation of GO hydrogels. The typical XRD (Figure S5, dominative) and SEM image (Figure 3D) reveal that the microstructure of the ion-induced hydrogel is similar to those of GO/polymer hydrogels. Because the metal ions alter little the pH value of GO solution, the coordination of metal ions with hydroxyl and carboxyl groups on GO sheets was considered to be the main driving force for the assembly of GO sheets. Multivalence transition-metal ions usually have larger coordination stability constants than those of alkali metal and alkaline-earth metal ions. Thus, the former ions also have stronger cross-linking abilities,

which were reflected by their smaller CGC values (caption of Figure 4). To confirm that metal ions acted as cross-linkers in the hydrogels, a chelating agent, ethylene diamine tetraacetic acid (EDTA), was added into the GO/metal hydrogel to remove metal ions.^{42,43} Upon addition of EDTA, the hydrogels decomposed quickly due to the loss of metal ions (Figure 6B). This phenomenon also confirmed that GO sheets contact with each other in their concentrated solution and small metal ions can interact with individual GO sheets to form 3D networks.

CONCLUSIONS

In conclusion, GO sheets with lateral dimensions of several micrometers are able to contact with each other to form a loose network in solution as their concentration is sufficiently high ($C_{GO} > 3 \text{ mg L}^{-1}$). The formation of the 3D network is because of the large and flexible 2D structure of GO sheets and the force balance between their static repulsion and bonding interaction. Increasing the bonding force or decreasing the repulsion force between GO sheets in solution will reinforce the 3D GO network and induce GO gelation or participation. These purposes can be realized by adding cross-linkers (polymers, small ammonium salts, and metal ions) or acidizing the GO solution. During the gelation and participation processes, many supramolecular interactions, such as hydrogen bonds, static or hydrophobic interactions, and coordination, are recognized as the possible driving forces. Careful control of the balance between electrostatic repulsion and bonding force is an important factor that governs the formation of GO hydrogels. All the GO hydrogels showed low critical gelation concentrations, and some of them exhibited environmental responsive behavior. This work indicates that GO is a good candidate for preparing “super” and “smart” hydrogels and will enlighten further studies on the supramolecular chemistry of graphene and its derivatives.

ASSOCIATED CONTENT

S Supporting Information. Dynamic rheological behavior of GO hydrogels and SEM images, XRD patterns, and photo images of lyophilized GO hydrogels. This material is available free of charge via the Internet at <http://pubs.acs.org>.

AUTHOR INFORMATION

Corresponding Author

*Phone: +86-10-6277-3743. Fax: +86-10-6277-1149. E-mail: gshi@tsinghua.edu.cn.

ACKNOWLEDGMENT

This work was supported by the Natural Science Foundation of China (50873052 and 91027028) and the China Postdoctoral Science Foundation (20090460027 and 201003100).

REFERENCES

- (1) Stankovich, S.; Dikin, D. A.; Piner, R. D.; Kohlhaas, K. A.; Kleinhammes, A.; Jia, Y.; Wu, Y.; Nguyen, S. T.; Ruoff, R. S. *Carbon* **2007**, *45*, 1558–1565.
- (2) Stankovich, S.; Piner, R. D.; Chen, X. Q.; Wu, N. Q.; Nguyen, S. T.; Ruoff, R. S. *J. Mater. Chem.* **2006**, *16*, 155–158.
- (3) Park, S.; Ruoff, R. S. *Nat. Nanotechnol.* **2009**, *4*, 217–224.
- (4) Bagri, A.; Mattevi, C.; Acik, M.; Chabal, Y. J.; Chhowalla, M.; Shenoy, V. B. *Nat. Chem.* **2010**, *2*, 581–587.
- (5) Paci, J. T.; Belytschko, T.; Schatz, G. C. *J. Phys. Chem. C* **2007**, *111*, 18099–18111.
- (6) Dreyer, D. R.; Park, S.; Bielawski, C. W.; Ruoff, R. S. *Chem. Soc. Rev.* **2010**, *39*, 228–240.
- (7) Liang, M. H.; Zhi, L. J. *J. Mater. Chem.* **2009**, *19*, 5871–5878.
- (8) Loh, K. P.; Bao, Q.; Eda, G.; Chhowalla, M. *Nat. Chem.* **2010**, *2*, 1015–1024.
- (9) Kim, J.; Cote, L. J.; Kim, F.; Yuan, W.; Shull, K. R.; Huang, J. *J. Am. Chem. Soc.* **2010**, *132*, 8180–8186.
- (10) Zhang, C.; Ren, L.; Wang, X.; Liu, T. *J. Phys. Chem. C* **2010**, *114*, 11435–11440.
- (11) Guo, P.; Song, H.; Chen, X. *J. Mater. Chem.* **2010**, *20*, 4867–4874.
- (12) Xu, Y. X.; Shi, G. Q. *J. Mater. Chem.* **2011**, *21*, 3311–3323.
- (13) Bai, H.; Li, C.; Shi, G. Q. *Adv. Mater.* **2011**, *23*, 1089–1115.
- (14) Cote, L. J.; Kim, F.; Huang, J. *J. Am. Chem. Soc.* **2008**, *131*, 1043–1049.
- (15) Medhekar, N. V.; Ramasubramaniam, A.; Ruoff, R. S.; Shenoy, V. B. *ACS Nano* **2010**, *4*, 2300–2306.
- (16) Dikin, D. A.; Stankovich, S.; Zimney, E. J.; Piner, R. D.; Dommett, G. H. B.; Evmenenko, G.; Nguyen, S. T.; Ruoff, R. S. *Nature* **2007**, *448*, 457–460.
- (17) Compton, O. C.; Nguyen, S. T. *Small* **2010**, *6*, 711–723.
- (18) Vickery, J. L.; Patil, A. J.; Mann, S. *Adv. Mater.* **2009**, *21*, 2180–2184.
- (19) Bai, H.; Li, C.; Wang, X. L.; Shi, G. Q. *Chem. Commun.* **2010**, *46*, 2376–2378.
- (20) Xu, Y. X.; Wu, Q.; Sun, Y. Q.; Bai, H.; Shi, G. Q. *ACS Nano* **2010**, *4*, 7358–7362.
- (21) Zu, S. Z.; Han, B. H. *J. Phys. Chem. C* **2009**, *113*, 13651–13657.
- (22) Wang, J. *ECS Trans.* **2009**, *19*, 241–247.
- (23) Tang, Z.; Shen, S.; Zhuang, J.; Wang, X. *Angew. Chem., Int. Ed.* **2010**, *49*, 4603–4607.
- (24) Xu, Y. X.; Sheng, K. X.; Li, C.; Shi, G. Q. *ACS Nano* **2010**, *4*, 4324–4330.
- (25) Worsley, M. A.; Pauzauskie, P. J.; Olson, T. Y.; Biener, J.; Satcher, J. H., Jr.; Baumann, T. F. *J. Am. Chem. Soc.* **2010**, *132*, 14067–14069.
- (26) Hummers, W. S.; Offeman, R. E. *J. Am. Chem. Soc.* **1958**, *80*, 1339–1339.
- (27) Xu, Y. X.; Bai, H.; Lu, G. W.; Li, C.; Shi, G. Q. *J. Am. Chem. Soc.* **2008**, *130*, 5856–5857.
- (28) Lerf, A.; He, H. Y.; Forster, M.; Klinowski, J. *J. Phys. Chem. B* **1998**, *102*, 4477–4482.
- (29) Gao, W.; Alemany, L. B.; Ci, L.; Ajayan, P. M. *Nat. Chem.* **2009**, *1*, 403–408.
- (30) Casabianca, L. B.; Shaibat, M. A.; Cai, W. W.; Park, S.; Piner, R.; Ruoff, R. S.; Ishii, Y. *J. Am. Chem. Soc.* **2010**, *132*, 5672–5676.
- (31) Li, D.; Müller, M. B.; Gilje, S.; Kaner, R. B.; Wallace, G. G. *Nat. Nanotechnol.* **2008**, *3*, 101–105.
- (32) Everett, D. H. *Basic Principles of Colloid Science*; The Royal Society of Chemistry: London, 1988.
- (33) Murata, K.; Aoki, M.; Suzuki, T.; Harada, T.; Kawabata, H.; Komori, T.; Ohseto, F.; Ueda, K.; Shinkai, S. *J. Am. Chem. Soc.* **1994**, *116*, 6664–6676.
- (34) Park, S.; Dikin, D. A.; Nguyen, S. T.; Ruoff, R. S. *J. Phys. Chem. C* **2009**, *113*, 15801–15804.
- (35) Putz, K. W.; Compton, O. C.; Palmeri, M. J.; Nguyen, S. T.; Brinson, L. C. *Adv. Funct. Mater.* **2010**, *20*, 3322–3329.
- (36) Kyotani, T.; Moriyama, H.; Tomita, A. *Carbon* **1997**, *35*, 1185–1187.
- (37) Qiu, L.; Yang, X.; Gou, X.; Yang, W.; Ma, Z. F.; Wallace, G.; Li, D. *Chem.—Eur. J.* **2010**, *16*, 10653–10658.
- (38) Kotov, N. A.; Dékány, I.; Fendler, J. H. *Adv. Mater.* **1996**, *8*, 637–641.
- (39) Wu, Q.; Xu, Y. X.; Yao, Z. Y.; Liu, A. R.; Shi, G. Q. *ACS Nano* **2010**, *4*, 1963–1970.
- (40) Xu, Y. X.; Zhao, L.; Bai, H.; Hong, W. J.; Li, C.; Shi, G. Q. *J. Am. Chem. Soc.* **2009**, *131*, 13490–13497.

- (41) Park, S.; Lee, K.-S.; Bozoklu, G.; Cai, W.; Nguyen, S. T.; Ruoff, R. S. *ACS Nano* **2008**, *2*, 572–578.
- (42) Chithra, P.; Varghese, R.; Divya, K. P.; Ajayaghosh, A. *Chem.—Asian J.* **2008**, *3*, 1365–1373.
- (43) Zhou, W.; Li, J.; He, X.; Li, C.; Lv, J.; Li, Y.; Wang, S.; Liu, H.; Zhu, D. *Chem.—Eur. J.* **2008**, *14*, 754–763.